Magazine of Civil Engineering. 2024. 17(5). Article No. 12901

Magazine of Civil Engineering

ISSN 2712-8172

journal homepage: http://engstroy.spbstu.ru/

Research article

UDC 624.012.45

DOI: 10.34910/MCE.129.1

Deformation of box-sectional structures during torsion with bending

N.I. Karpenko [1], ***S.N. Karpenko*** [1], ***Vl.I. Kolchunov*** [2], ***V.I. Kolchunov*** [2] ✉

[1] *Research Institute of Building Physics (NIISF RAACS), Moscow, Russian Federation*

[2] *Moscow State University of Civil Engineering (National Research University), Moscow, Russian Federation*

✉ *asiorel@mail.ru*

Keywords: reinforced concrete, torsion, bending moment, axial load, combined action, box section

Abstract. The article is devoted to the problem of complex stress state of reinforced concrete under the action of torsion with bending, taking into account axial and transverse forces. The existing calculation models remain imperfect, despite a significant number of publications in the world on this problem. They are fragmentary and sometimes contradictory and consider individual special cases of stress. The proposed version of the deformation model is based on physical relations for reinforced concrete, static equations and conditions for compatibility of deformations in the design section at the stage after the crack formation. The calculation model takes into account all the components of external forces in the rod element, the spatial nature of cracks, various cases of the location of the compressed concrete zone or its absence, depending on the ratio of the acting forces in the design structure. The obtained analytical dependences allow one to determine interconnected design parameters, such as stresses in the concrete of the compressed zone, the height of the compressed concrete, stresses in axial and transverse rods, deformations in concrete and reinforcement, curvature and twisting angle of a reinforced concrete element, while simultaneously applying a twisting and bending moments, axial and transverse forces to the element. The deformation model obtained in the article can be used in the design of a wide class of reinforced concrete structures under the action of torsion with bending taking into account axial and transverse forces in the calculated element.

Citation: Karpenko, N.I., Karpenko, S.N., Kolchunov, Vl.I., Kolchunov, V.I. Deformation of box-sectional structures during torsion with bending. Magazine of Civil Engineering. 2024. 17(6). Article no. 13001. DOI: 10.34910/MCE.130.1

1. *Introduction*

Reinforced concrete structures of civil and industrial buildings and structures are considered as an object of study undergoing a complex stress state – torsion with bending, taking into account axial and transverse forces.

Calculation of such structures remains one of the byways of the theory of reinforced concrete. It is suffice to note that up until now, in foreign and Russian guidelines on the design of reinforced concrete structures and in scientific publications of the last decade, for example, [1–7] and others, conditional design models are used, including even truss analogy models [8–11]. Experimental studies of such structures were few and they were also fragmentary in the study of individual cases and types of the deformed state, cracking and destruction of complexly stressed structures, for example, with the overrepresentation of bending [5, 12, 13], with the overrepresentation of torsion without regard to transverse forces, torsion with bending in the horizontal plane [14], studies of structures reinforced with an external cage [15, 16] and models of transverse and torsional stability [17], and others. So far, there are no general analytical methods for modeling complexly stressed reinforced concrete structures under the considered stress state, despite the fact that attempts to create them have been made repeatedly. One of the most general calculation models of deformation of reinforced concrete with cracks in a complex stress state is based on the section method and is being developed in Russia. It includes the deformation model of N.I. Karpenko [18] and a block deformation model with a spatial calculated section with a wide range of design parameters taken into account [19]. These models are increasingly receiving experimental substantiation at various ratios, different shapes and structures of sections and for different classes of concrete [20–22].

Numerical methods are used to solve the class of problems under consideration, in particular, the finite element method implemented in software systems [23–25]. An analysis of their application shows [26] that they not only do not allow a qualitative analysis of the studied physical parameters during the deformation of reinforced concrete with cracks but also relatively approximately describe the results of experimental studies of reinforced concrete structures under the considered stress state and, especially, the parameters of the limit states of the second group, for example, crack opening width in structures made of high-strength reinforced concrete and fiber-reinforced concrete [16].

In all known analytical models, including those proposed by the authors [18, 27], cases of a complex stress state are considered, when in a spatial section, not a through crack is formed but a crack that is interrupted in the compressed zone of concrete. In this regard, the article under consideration presents the features of constructing a design model for box-sectional elements under the combined action of bending and torque moments, normal and tangential forces for areas of a reinforced concrete element with through cracks. This case is realized when the element is dominated by bending with torsion and the normal longitudinal tensile force.

The relevance of such a study is determined by the increasingly complex types of impacts on reinforced concrete structures and the need to take them into account when designing buildings and structures to improve their safety.

The aim of the study was to determine the stress-strain state of reinforced concrete box-sectional structures during torsion with bending under the action of transverse and tensile longitudinal forces in the design section.

The tasks of the study were as follows:

- construction of a design scheme for reinforced concrete structures of rectangular box-shaped and solid sections with spatial cracks;
- determination of forces in longitudinal and transverse reinforcement;
- determination of deformations in the lower and upper zones as well as the side walls of the cross-sectional box of the element.

2. Methods

2.1. Scheme of the Reinforcement of a Cross-Sectional Box Element

The cross-sectional box of the reinforced element of size $h \times b$ is reinforced with four longitudinal reinforcement rods. Two rods (1, 2) with area $F_{S(1)}$ and $F_{S(2)}$ are located in the lower tension zone and two rods (3, 4) with area $F'_{S(3)}$ and $F'_{S(4)}$ – in the upper tension zone. We assume that $F'_{S(3)} = F'_{S(4)} = F'_S$, h_1, b_1 is the distance between the rods.

Longitudinal reinforcement is bordered by closed clamps with area F_{SW0} and the pitch U_{SW0}; h_2 and b_2 are the dimensions of the clamps. The clamps are transferred to the level of the longitudinal reinforcement with a reduced pitch U_{SW} as in the more general model, where

$$U_{SW} = U_{SW0} \frac{\left(b_1 + h_1\right)}{\left(b_2 + h_2\right)}. \tag{1}$$

The running area of the clamps will be:

$$f_{SW} = \frac{F_{SW0}}{U_{SW}} = F_{SW0} \frac{(b_2 + h_2)}{(b_1 + h_1) U_{SW0}}. \quad (2)$$

2.2. The Tangential Force Flows

The design diagram of the cross-sectional box of the element with through cracks is shown in Fig. 1. This diagram is realized when the torques (T) and normal tensile force (N) are predominant. The action of tangential forces is reduced to the flow of tangential forces along the contour 1–2–3–4 (Fig. 2a).

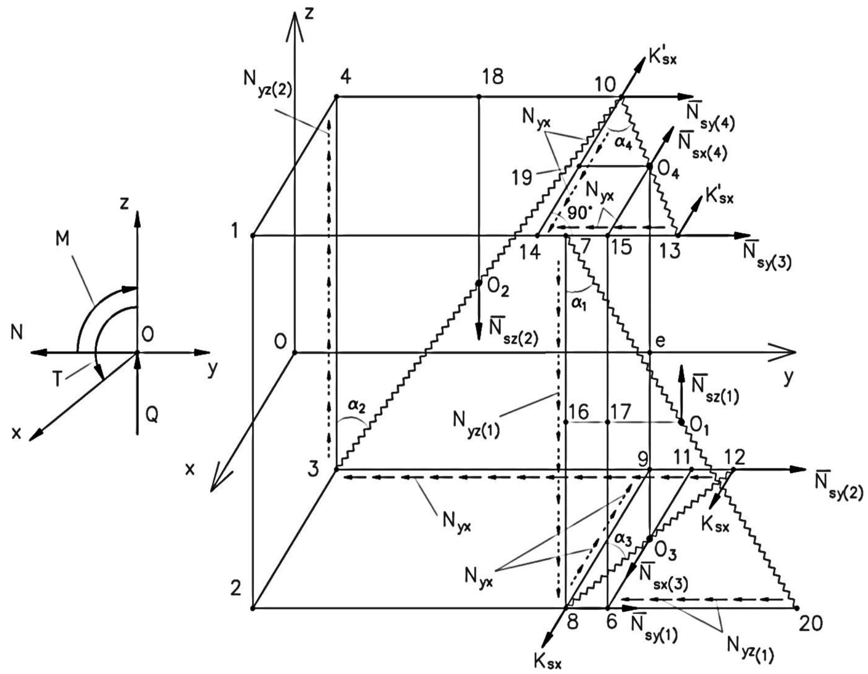

Figure 1. Design diagram of the cross-sectional box with through cracks.

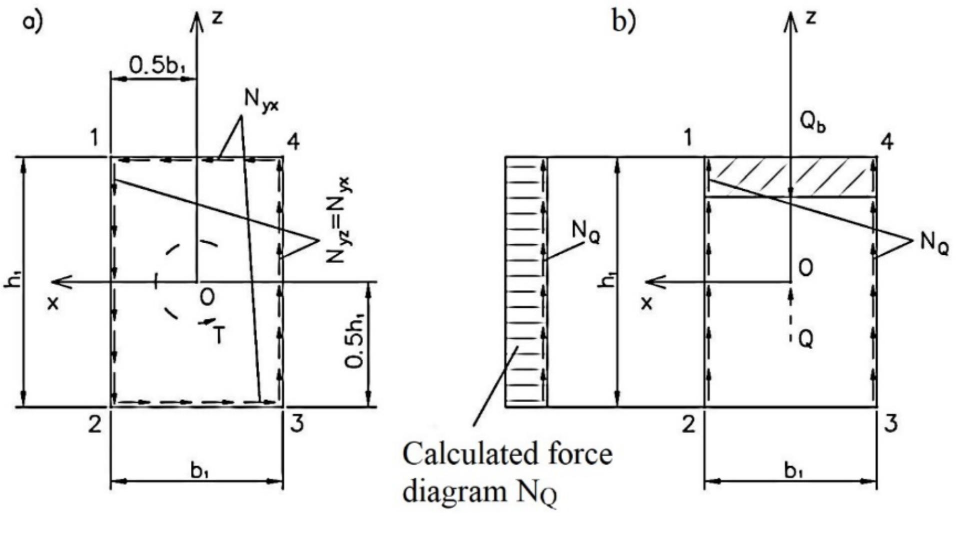

Figure 2. a) – scheme of tangential force flows N_{yx}, N_{zy} from the action of the torque T along the design contours 1–2–3–4; b) – flow diagrams of tangential forces from N_Q from the action of the tangential force along the design contours 1–2–3–4.

$$N_{yx} = N_{yz} = \frac{T}{2h_1b_1}. \quad (3)$$

The action of tangential forces is reduced to flows

$$N_Q = \frac{Q}{2h_1}. \tag{4}$$

The total flow on line 1–2 will be

$$N_{yz(1)} = \frac{T}{2h_1b_1} - \frac{Q}{2h_1}. \tag{5}$$

The total flow on line 3–4 will be

$$N_{yz(2)} = \frac{T}{2h_1b_1} + \frac{Q}{2h_1}. \tag{6}$$

The flows of tangential forces along lines 2–3 and 1–4 will be equal to the values of N_{yx}, determined by dependence (3).

2.3. Determination of Forces and Stresses in Transverse Reinforcement Rods

Inclined lines 7–20 and 3–10 pass along inclined cracks located in the vertical walls of the cross-sectional box of the element, $\overline{N}_{sz(1)}$ and $\overline{N}_{sz(2)}$ are the total forces taken by the vertical rods of the clamps in these walls.

The angles of inclination of cracks in vertical walls approach 45°. In this case, the effect of dowel forces is reduced. In this regard, the vertical thrust forces in the longitudinal reinforcement are neglected. As a result, considering the conditions for the balance of forces in elements 3–4–10 and 8–7–20 from the action of torques, we find that the forces $\overline{N}_{sz(1)}$ and $\overline{N}_{sz(2)}$, perceived, respectively, in inclined cracks 7–20 and 3–10, will be:

$$\begin{aligned} \overline{N}_{sz(1)} &= N_{yz(1)}l_{7-8} = N_{yz(1)}h_1; \\ \overline{N}_{sz(2)} &= N_{yz(2)}l_{3-4} = N_{yz(2)}h_1. \end{aligned} \tag{7}$$

The forces $\overline{N}_{sz(1)}$ and $\overline{N}_{sz(2)}$ are expressed through the stresses $\sigma_{sz(1)}$ and $\sigma_{sz(2)}$ in the vertical rods of the clamps located along lines 7–8 and 4–3 in sections 8–20 and 4–10, respectively,

$$\begin{aligned} \overline{N}_{sz(1)} &= N_{yz(1)}l_{7-8} = \sigma_{sz(1)}h_1\text{tg}\alpha_1 f_{SW}; \\ \overline{N}_{sz(2)} &= N_{yz(2)}l_{3-4} = \sigma_{sz(2)}h_1\text{tg}\alpha_2 f_{SW}, \end{aligned} \tag{8}$$

where:

$$\begin{aligned} \sigma_{sz(1)} &= \frac{N_{yz(1)}}{\text{tg}\alpha_1 f_{SW}} = \left(\frac{T}{2h_1b_1} - \frac{Q}{2h_1}\right)\frac{1}{f_{SW}\text{tg}\alpha_1}; \\ \sigma_{sz(2)} &= \frac{N_{yz(2)}}{\text{tg}\alpha_2 f_{SW}} = \left(\frac{T}{2h_1b_1} - \frac{Q}{2h_1}\right)\frac{1}{f_{SW}\text{tg}\alpha_2}. \end{aligned} \tag{9}$$

Now we will have to determine the stresses in the rods located in the lower and upper walls of the box-section of the element. The inclined lines 8–12 and 10–13 (Fig. 1) pass along the cracks that intersect the lower and upper walls of the cross-sectional box of the element, where $\overline{N}_{SX(3)}$ and $\overline{N}_{SX(4)}$ are the total forces, perceived by the clamps, respectively, in cracks 8–12 and 10–13. According to the design scheme (Fig. 1), these efforts will be equal:

$$\begin{aligned} \overline{N}_{SX(3)} &= N_{yx}l_{8-9} - 2k_{SX} = N_{yx}b_1 - 2k_{SX}; \\ \overline{N}_{SX(4)} &= N_{yx}l_{10-14} - 2k'_{SX} = N_{yx}b_1 - 2k'_{SX}. \end{aligned} \tag{10}$$

Following [18], the influence of the dowel conditions k_{SX} and k'_{SX} can be taken into account using the coefficients λ_x and λ'_x. In this case, dependencies (10) are transformed into the form:

$$\begin{aligned}\bar{N}_{SX(3)} &= N_{yx}b_1 - 2k_{SX} = N_{yx}b_1\lambda_x;\\ \bar{N}_{SX(4)} &= N_{yx}b_1 - 2k'_{SX} = N_{yx}b_1\lambda'_x,\end{aligned} \tag{11}$$

where

$$\begin{aligned}\lambda_x &= \frac{15f_{SW}}{15f_{SW} + f_{Sy}\mathrm{ctg}^2\alpha_3};\\ \lambda'_x &= \frac{15f_{SW}}{15f_{SW} + f'_{Sy}\mathrm{ctg}^2\alpha_4},\end{aligned} \tag{12}$$

at

$$\begin{aligned}f_{SY} &= \frac{F_{sy(1)} + F_{sy(2)}}{b_1};\\ f'_{SY} &= \frac{F'_{sy(1)} + F'_{sy(2)}}{b_1}.\end{aligned} \tag{13}$$

The forces $\bar{N}_{SX(3)}$ and $\bar{N}_{SX(4)}$ are expressed through the stresses σ_{sx} and σ'_{sx}, respectively, in the lower and upper rods of the clamps.

$$\begin{aligned}\bar{N}_{SX(3)} &= N_{yx}b_1\lambda_x = \sigma_{sx}f_{sw}l_{9-12} = \sigma_{sx}f_{sw}b_1\mathrm{tg}\alpha_3;\\ \bar{N}_{SX(4)} &= N_{yx}b_1\lambda'_x = \sigma'_{sx}f_{sw}l_{14-13} = \sigma'_{sx}f_{sw}b_1\mathrm{tg}\alpha_4.\end{aligned} \tag{14}$$

Where, taking into account the values of N_{yx}, determined by the formula (3):

$$\begin{aligned}\sigma_{sx} &= \frac{N_{yx}\lambda_x}{f_{sw}\mathrm{tg}\alpha_3} = \frac{T\lambda_x}{2\left(b_1 + h_1\right)f_{sw}\mathrm{tg}\alpha_3};\\ \sigma'_{sx} &= \frac{N_{yx}\lambda'_x}{f_{sw}\mathrm{tg}\alpha_4} = \frac{T\lambda'_x}{2\left(b_1 + h_1\right)f_{sw}\mathrm{tg}\alpha_4}.\end{aligned} \tag{15}$$

From (11) the values also follow:

$$\begin{aligned}k_{SX} &= \frac{N_{yx}b_1\left(1-\lambda_x\right)}{2} = \frac{T}{2h_1}\left(1-\lambda_x\right);\\ k'_{SX} &= \frac{N_{yx}b_1\left(1-\lambda'_x\right)}{2} = \frac{T}{2h_1}\left(1-\lambda'_x\right).\end{aligned} \tag{16}$$

2.4. Determination of Normal Stresses in Longitudinal Reinforcement Rods

In the design scheme shown in Fig. 1, we select the plane $6-15-\mathrm{O}_4-\mathrm{O}_3$, parallel to the plane ZOY, respectively, the normal plane XOZ and its two lines $15-\mathrm{O}_4$ and $6-\mathrm{O}_3$, located on the upper and lower surfaces of the box section.

The sum of the moments of all forces acting parallel to the plane ZOY relative to the upper line $15-\mathrm{O}_4$ will be equal to:

$$\begin{gathered}\bar{N}_{SY(1)}h_1+\bar{N}_{SY(2)}h_1-N_{YZ(1)}h_1l_{8-20}+\bar{N}_{SZ(1)}l_{17-O_1}+\\+\bar{N}_{SZ(2)}\left(l_{18-10}+l_{14-15}\right)-N_{YX(1)}l_{3-12}h_1-\\-\left(M+0.5Nh_1+Ql_{0-e}\right)=0\end{gathered}\qquad(17)$$

or, taking into account dependence (7), and

$$\begin{gathered}l_{17-O_1}=\left(0.5h_1\mathrm{tg}\alpha_1-0.5b_1\mathrm{tg}\alpha_3\right);\\l_{18-10}=0.5h_1\mathrm{tg}\alpha_2;\\l_{14-15}=0.5b_1\mathrm{tg}\alpha_4;\\l_{3-12}=0.5h_1\mathrm{tg}\alpha_2+0.5b_1\mathrm{tg}\alpha_4+0.5b_1\mathrm{tg}\alpha_3;\\l_{0-e}=h_1\mathrm{tg}\alpha_2+0.5b_1\mathrm{tg}\alpha_4;\\l_{8-20}=h_1\mathrm{tg}\alpha_1;\\M+Ql_{0-e}=M_e,\end{gathered}\qquad(18)$$

where M_e is the moment applied at point e of the plane $6-15-\mathrm{O}_4-\mathrm{O}_3,$ we find:

$$\begin{gathered}\left(\bar{N}_{SY(1)}+\bar{N}_{SY(2)}\right)=\frac{M_e+0.5Nh_1}{h_1}+N_{YZ(1)}h_1\mathrm{tg}\alpha_1-0.5N_{YZ(1)}\left(h_1\mathrm{tg}\alpha_1-b_1\mathrm{tg}\alpha_3\right)+\\+0.5N_{YZ(2)}\left(h_1\mathrm{tg}\alpha_2+b_1\mathrm{tg}\alpha_4\right)+0.5N_{YX(1)}\left(h_1\mathrm{tg}\alpha_2+0.5b_1\mathrm{tg}\alpha_4+0.5b_1\mathrm{tg}\alpha_3\right),\end{gathered}\qquad(19)$$

or

$$\begin{gathered}\bar{N}_{SY(1)}+\bar{N}_{SY(2)}=\frac{M_e+0.5Nh_1}{h_1}+0.5N_{YZ(1)}\left(h_1\mathrm{tg}\alpha_1+b_1\mathrm{tg}\alpha_3\right)-\\-0.5N_{YZ(2)}\left(h_1\mathrm{tg}\alpha_2+b_1\mathrm{tg}\alpha_4\right)+N_{YX(1)}\left(h_1\mathrm{tg}\alpha_2+0.5b_1\mathrm{tg}\alpha_4+0.5b_1\mathrm{tg}\alpha_3\right).\end{gathered}\qquad(20)$$

In the case of pure torsion,

$$\begin{gathered}\left(\bar{N}_{SY(1)}+\bar{N}_{SY(2)}\right)=\\=N_{YX(1)}\left(0.5h_1+0.5b_1-0.5b_1-0.5h_1+h_1+0.5b_1+0.5b_1\right)=0,\end{gathered}\qquad(21)$$

or

$$\bar{N}_{SY(1)}+\bar{N}_{SY(2)}=\left(h_1+b_1\right)N_{YX}.\qquad(22)$$

To determine the relationship between the forces $\bar{N}_{SY(1)}$ and $\bar{N}_{SY(2)},$ we use the condition that the sum of the torques of all forces in the reinforcement and concrete of the design element is equal to zero relative to the $\mathrm{O}_4-\mathrm{O}_3$ axis. In this case, we assume that some influence of the difference in efforts $\bar{N}_{SY(3)}$ and $\bar{N}_{SY(4)}$ can be neglected, assuming that

$$\bar{N}_{SY(3)}\approx\bar{N}_{SY(4)}.\qquad(23)$$

In this case, the sum of the moments of all forces applied in the sections of the design scheme (Fig. 1) relative to the vertical line $\mathrm{O}_4-\mathrm{O}_3$ is equal to zero and can be represented as:

$$\bar{N}_{SY(1)} l_{6-\mathrm{O}_3} - \bar{N}_{SY(2)} l_{11-\mathrm{O}_3} + \bar{N}_{SY(3)} l_{15-\mathrm{O}_4} - \bar{N}_{SY(4)} l_{19-10} + N_{YX} l_{3-12} l_{11-\mathrm{O}_3} -$$
$$- N_{YX} l_{7-13} l_{15-\mathrm{O}_4} - N_{YZ(1)} l_{8-20} l_{6-\mathrm{O}_3} + k_x l_{8-6} - k_x l_{11-12} = 0,$$

where:

$$l_{6-\mathrm{O}_3} = l_{11-\mathrm{O}_3} + l_{15-\mathrm{O}_4} - l_{19-10} = \frac{b_1}{2};$$
$$l_{3-12} = h_1 \mathrm{tg}\alpha_2 + 0.5\left(b_1 \mathrm{tg}\alpha_4 + b_1 \mathrm{tg}\alpha_3\right);$$
$$l_{7-13} = 0.5\left(b_1 \mathrm{tg}\alpha_4 + b_1 \mathrm{tg}\alpha_3\right);$$
$$l_{8-20} = h_1 \mathrm{tg}\alpha_1;$$
$$l_{8-6} = l_{11-12} = 0.5 b_1 \mathrm{tg}\alpha_3.$$

As a result, the sum of the moments relative to the $\mathrm{O}_4 - \mathrm{O}_3$ line is converted to the form:

$$\begin{gathered}\left(\bar{N}_{SY(1)} - \bar{N}_{SY(2)} + \bar{N}_{SY(3)} - \bar{N}_{SY(4)}\right)0.5b_1 + \\ + N_{YX}\left(h_1 \mathrm{tg}\alpha_2 + 0.5b_1 \mathrm{tg}\alpha_4 + 0.5b_1 \mathrm{tg}\alpha_3 - 0.5b_1 \mathrm{tg}\alpha_4 - 0.5b_1 \mathrm{tg}\alpha_3\right)0.5b_1 - \\ - N_{YZ(1)} h_1 \mathrm{tg}\alpha_1 0.5b_1 + k_x\left(0.5b_1 \mathrm{tg}\alpha_3 - 0.5b_1 \mathrm{tg}\alpha_3\right) + k'_{sx}\left(0.5b_1 \mathrm{tg}\alpha_4 - 0.5b_1 \mathrm{tg}\alpha_4\right) = 0,\end{gathered} \tag{24}$$

where, taking into account condition (23), it follows:

$$\bar{N}_{SY(1)} - \bar{N}_{SY(2)} = N_{YZ(1)} h_1 \mathrm{tg}\alpha_1 - N_{YX(1)} h_1 \mathrm{tg}\alpha_2$$

or

$$\bar{N}_{SY(1)} = \bar{N}_{SY(2)} + N_{YZ(1)} h_1 \mathrm{tg}\alpha_1 - N_{YX(1)} h_1 \mathrm{tg}\alpha_2. \tag{25}$$

Substituting the value $\bar{N}_{SY(1)}$ into (20), we find:

$$\bar{N}_{SY(2)} = \frac{M_e + 0.5Nh_1}{2h_1} - 0.25N_{YZ(1)}\left(h_1 \mathrm{tg}\alpha_1 - b_1 \mathrm{tg}\alpha_3\right) -$$
$$-0.25N_{YZ(2)}\left(h_1 \mathrm{tg}\alpha_2 + b_1 \mathrm{tg}\alpha_4\right) + N_{YX(1)}\left(h_1 \mathrm{tg}\alpha_2 + 0.25b_1 \mathrm{tg}\alpha_3 + 0.25b_1 \mathrm{tg}\alpha_4\right),$$

or, taking into account (3), (5) and (6):

$$\begin{gathered}\bar{N}_{SY(2)} = \frac{M_e + 0.5Nh_1}{2h_1} - \left(\frac{T}{8b_1h_1} - \frac{Q}{8h_1}\right)\left(h_1 \mathrm{tg} \propto_1 - b_1 \mathrm{tg} \propto_3\right) - \\ - \left(\frac{T}{8b_1h_1} + \frac{Q}{8h_1}\right)\left(h_1 \mathrm{tg} \propto_2 + b_1 \mathrm{tg} \propto_4\right) + \frac{T}{2b_1h_1}\left(h_1 \mathrm{tg} \propto_2 + 0.25b_1 \mathrm{tg} \propto_3 + 0.25b_1 \mathrm{tg} \propto_4\right).\end{gathered} \tag{26}$$

Substitution of $\bar{N}_{SY(2)}$ into (25) leads to the dependence

$$\bar{N}_{SY(1)} = \frac{M_e + 0.5Nh_1}{2h_1} + N_{YZ(1)}\left(0.75h_1 \mathrm{tg}\alpha_1 + 0.25b_1 \mathrm{tg}\alpha_3\right) -$$
$$-0.25N_{YZ(2)}\left(h_1 \mathrm{tg}\alpha_2 + b_1 \mathrm{tg}\alpha_4\right) + 0.25N_{XY}\left(b_1 \mathrm{tg}\alpha_3 + b_1 \mathrm{tg}\alpha_4\right),$$

or, taking into account (3), (5) and (6),

$$\bar{N}_{SY(1)} = \frac{M_e + 0.5Nh_1}{2h_1} - \left(\frac{T}{8b_1h_1} - \frac{Q}{8h_1}\right)\left(3h_1 \operatorname{tg} \propto_1 + b_1 \operatorname{tg} \propto_3\right) - \\ - \left(\frac{T}{8b_1h_1} + \frac{Q}{8h_1}\right)\left(h_1 \operatorname{tg} \propto_2 + b_1 \operatorname{tg} \propto_4\right) + \frac{T}{8h_1}\left(\operatorname{tg} \propto_3 + \operatorname{tg} \propto_4\right). \quad (27)$$

Let us proceed to the determination of the forces $\bar{N}_{SY(3)}$ and $\bar{N}_{SY(4)}$ in the longitudinal reinforcement. The sum of the moments of all efforts applied to the right side of the design model relative to the lower line 6–11 will be equal to:

$$\bar{N}_{SY(3)}h_1 + \bar{N}_{SY(4)}h_1 - N_{YX}l_{7-13}h_1 - \bar{N}_{SZ(1)}l_{17-O_1} - \bar{N}_{YZ(2)}\left(0.5h_1 \operatorname{tg} \propto_2 + 0.5b_1 \operatorname{tg} \propto_4\right) \\ = -M + 0.5Nh_1 - Ql_{0-e} = -M_e + 0.5Nh_1,$$

or, taking into account the values of $\bar{N}_{SZ(1)}$ and $\bar{N}_{SZ(2)}$, determined by formulas (7), and condition (23), we find:

$$\bar{N}_{SY(3)} = \bar{N}_{SY(4)} = \frac{0.5Nh_1 - M_e}{2h_1} + 0.25N_{YX}\left(b_1 \operatorname{tg}\alpha_4 + b_1 \operatorname{tg}\alpha_3\right) + \\ + 0.25N_{YZ(1)}\left(h_1 \operatorname{tg}\alpha_1 + b_1 \operatorname{tg}\alpha_3\right) + 0.25N_{YZ(2)}\left(h_1 \operatorname{tg}\alpha_2 + b_1 \operatorname{tg}\alpha_4\right),$$

or, taking into account (3), (5) and (6):

$$\bar{N}_{SY(3)} = \bar{N}_{SY(4)} = \frac{0.5Nh_1 - M_e}{2h_1} + \frac{T}{8h_1}\left(\operatorname{tg} \propto_4 + \operatorname{tg} \propto_3\right) + \\ + \left(\frac{T}{8b_1h_1} - \frac{Q}{8h_1}\right)\left(h_1 \operatorname{tg} \propto_1 - b_1 \operatorname{tg} \propto_3\right) + \left(\frac{T}{8b_1h_1} + \frac{Q}{8h_1}\right)\left(h_1 \operatorname{tg} \propto_3 + b_1 \operatorname{tg} \propto_4\right). \quad (28)$$

After determining the forces $\bar{N}_{SZ(1)}$, $\bar{N}_{SZ(2)}$, $\bar{N}_{SZ(3)}$ in the reinforcement, we determine the stresses in the reinforcement:

$$\sigma_{sy(1)} = \frac{\bar{N}_{sy(1)}}{F_{s(1)}};$$

$$\sigma_{sy(2)} = \frac{\bar{N}_{sy(2)}}{F_{s(2)}};$$

$$\sigma_{sy(3)} = \frac{\bar{N}_{sy(3)}}{F'_{s(3)}}; \quad (29)$$

$$\sigma_{sy(4)} = \frac{\bar{N}_{sy(4)}}{F'_{s(4)}}.$$

2.5. Determination of Deformations in the Lower and Upper Zones of the Element

Average relative deformations in rods 1 and 2 of the lower longitudinal reinforcement in the sections between cracks are determined by the dependencies:

$$\varepsilon_{SY(1)} = \frac{\sigma_{sy(1)}\psi_{sy(1)}}{E_S} = \frac{\bar{N}_{sy(1)}\psi_{sy(1)}}{E_S F_{s(1)}};$$
$$\varepsilon_{SY(2)} = \frac{\sigma_{sy(2)}\psi_{sy(2)}}{E_S} = \frac{\bar{N}_{sy(2)}\psi_{sy(2)}}{E_S F_{s(2)}}, \tag{30}$$

where $\psi_{sy(1)}$, $\psi_{sy(2)}$ are coefficients that take into account the effect of adhesion of reinforcement to concrete in the sections between cracks (V.I. Murashev's coefficients), $\sigma_{sy(1)}$ and $\sigma_{sy(2)}$ are stresses in rods 1 and 2 in cracks, determined from dependencies (26), (29),

$$\psi_{sy(1)} = 1 - 0.75\varphi_S \frac{\sigma_{cnc}}{\sigma_{sy(1)}};$$
$$\psi_{sy(1)} = 1 - 0.75\varphi_S \frac{\sigma_{cnc}}{\sigma_{sy(2)}}, \tag{31}$$

where σ_{cnc} are stresses in the reinforcement at the moment of cracking, which in the first approximation can be determined by the formula:

$$\sigma_{cnc} = \frac{2.5R_{btser}\mathrm{E}_s}{E_b}, \tag{32}$$

φ_S = 1 – with short-term load, φ_S = 0.8 – with prolonged action of the load. The calculation includes the average deformations of the two lower reinforcement rods

$$\varepsilon_{SY} = \frac{\varepsilon_{SY(1)} + \varepsilon_{SY(2)}}{2},$$

or given (30),

$$\varepsilon_{sy} = \frac{1}{2E_S}\left(\frac{\bar{N}_{sy(1)}\varphi_{sy(1)}}{F_{S(1)}} + \frac{\bar{N}_{sy(2)}\varphi_{sy(2)}}{E_{S(2)}}\right). \tag{33}$$

By analogy with (33), the average deformations of the upper longitudinal reinforcement will be equal to:

$$\varepsilon'_{SY} = \frac{1}{2E_S}\left(\frac{\bar{N}_{sy(3)}\varphi_{sy(3)}}{F_{S(1)}} + \frac{\bar{N}_{sy(4)}\varphi_{sy(4)}}{E_{S(4)}}\right), \tag{34}$$

where $\varphi_{sy(3)}$, $\varphi_{sy(4)}$ are determined by formula (31), where indices 1 and 2 are replaced by indices 3 and 4.

The average value of the deformations of the clamps in the lower and upper walls of the cross-sectional box of the element by analogy with (30) – (32) and taking into account (15) will be:

$$\varepsilon_{SX} = \frac{\sigma_{sx}\psi_{sx}}{E_S} = \frac{N_{yx}\lambda_x\varphi_{sx}}{f_{sw}E_S\,\mathrm{tg}\lambda_3}. \tag{35}$$

By analogy with (35), the average strains of the clamps in the upper wall of the cross-sectional box of the element will be equal to the upper longitudinal reinforcement will be equal:

$$\varepsilon'_{SX} = \frac{\sigma'_{sx}\psi'_{sx}}{E_S} = \frac{N_{yx}\lambda'_x\varphi'_{sx}}{f_{sw}E_S\,\mathrm{tg}\lambda_3}. \tag{36}$$

Introducing into (33), (36) the values $\bar{N}_{sy(1)}$, $\bar{N}_{sy(2)}$, $\bar{N}_{sy(3)}$, $\bar{N}_{sy(4)}$, N_{yx} from (26) – (28) and (3), we obtain the values ε_{SY}, ε'_{SY}, ε_{SX}, ε'_{SX} as a function of M, N, T, Q.

In the future, stresses σ_{bt} and σ'_{bt} and deformations ε_{bt}, ε'_{bt}, respectively, in the lower and upper walls of the element will also be needed. These deformations will mainly depend on the shear stresses τ_{yx} and τ'_{yx}.

$$\begin{aligned} \sigma_{bt} &\approx -2_{yx}\sin\alpha_3\cos\alpha_3; \\ \sigma'_{bt} &\approx -2'_{yx}\sin\alpha_4\cos\alpha_4; \end{aligned} \tag{37}$$

$$\begin{aligned} \varepsilon_{bt} &= \frac{\sigma_{bt}}{E_n\nu_{nx}} = \frac{-2_{yx}\sin\alpha_3\cos\alpha_3}{E_n\nu_{nx}}; \\ \varepsilon'_{bt} &= \frac{\sigma'_{bt}}{E'_n\nu'_{nx}} = \frac{-2'_{yx}\sin\alpha_4\cos\alpha_4}{E'_n\nu'_{nx}}, \end{aligned} \tag{38}$$

where E_n, E'_n are modules of deformation of concrete strips

$$E_n = E'_n = E_b\beta_n \approx 0.8E_b, \tag{39}$$

$\beta_n \approx 0.8$ is coefficient of influence of loosening of concrete strips with cracks and reduction of modulus, ν_{nx} is coefficient taking into account the effect of plastic deformations of concrete strips on the increase in deformations ε_{bt} is determined from the dependence (2), (3). Shear stresses are determined depending on the linear shear forces N_{yx}.

$$\begin{aligned} \tau_{yx} &= \frac{N_{yx}}{2a\beta_{xy}}; \\ \sigma_{bt} &= \frac{-2N_{yx}\sin\alpha_3\cos\alpha_3}{2a\beta_{xy}}; \\ \tau'_{yx} &= \frac{N_{yx}}{2a\beta'_{xy}}; \\ \sigma'_{bt} &= \frac{-2N_{yx}\sin\alpha_4\cos\alpha_4}{2a\beta'_{xy}}, \end{aligned} \tag{40}$$

where a is concrete cover, β_{xy}, β'_{xy} are the coefficients of influence of the remaining concrete layers on the values τ_{yx}, τ'_{xy}, a "–" sign means that the stripes are decreasing. Taking into account (37), (39):

$$\begin{aligned} \varepsilon_{bt} &= \frac{-2N_{yx}\sin\alpha_3\cos\alpha_3}{2\alpha\beta_{xy}E_n\beta_n\nu_{nx}} = -\frac{2N_{yx}\sin\alpha_3\cos\alpha_3}{2aE_b\tilde{\nu}_{nx}}; \\ \varepsilon'_{bt} &= \frac{-2N_{yx}\sin\alpha_4\cos\alpha_4}{2\alpha\beta'_{xy}E_n\beta_n\nu'_{nx}} = -\frac{2N_{yx}\sin\alpha_4\cos\alpha_4}{2aE_b\tilde{\nu}'_{nx}}, \end{aligned} \tag{41}$$

where

$$\begin{aligned} \tilde{\nu}_{nx} &= \beta_n\nu_{nx}\beta_{xy}; \\ \tilde{\nu}'_{nx} &= \beta_n\nu'_{nx}\beta'_{xy}. \end{aligned} \tag{42}$$

The coefficients ν_{nx} and ν'_{nx} are determined experimentally.

Following [18] and taking into account (33) – (35), the shear angles in the lower and upper horizontal walls of the cross-sectional box of the element will be equal:

$$\gamma_{SY} = \varepsilon_{SX}\operatorname{ctg}\alpha_3 + \varepsilon_{SY}\operatorname{tg}\alpha_3 - \frac{\varepsilon_{bt}}{\sin\alpha_3\cos\alpha_3} =$$

$$= \frac{N_{yx}\lambda_x\varphi_{sx}}{f_{sw}E_S\operatorname{tg}\lambda_3}\operatorname{ctg}\alpha_3 + \frac{1}{2E_S}\left(\frac{\bar{N}_{sy(1)}\varphi_{sy(1)}}{F_{S(1)}} + \frac{\bar{N}_{sy(2)}\varphi_{sy(2)}}{F_{S(4)}}\right)\operatorname{tg}\alpha_3 + \frac{N_{yx}}{\alpha E_b\tilde{\nu}_{nx}}; \quad (43)$$

$$\gamma'_{SY} = \frac{N_{yx}\lambda'_x\varphi'_{sx}}{f_{sw}E_S\operatorname{tg}\lambda_4}\operatorname{ctg}\alpha_4 + \frac{1}{2E_S}\left(\frac{\bar{N}_{sy(3)}\varphi_{sy(3)}}{F_{S(3)}} + \frac{\bar{N}_{sy(4)}\varphi_{sy(4)}}{F_{S(4)}}\right)\operatorname{tg}\alpha_4 - \frac{N_{yx}}{\alpha E_b\tilde{\nu}'_{nx}}.$$

2.6. Determination of the Deformations of the Side Walls of the Cross-Sectional Box of the Element

There are four types of relative deformations: average relative deformations of longitudinal reinforcement $\varepsilon_{y(1)}$ – in the first vertical wall with 1, 3 longitudinal bars and $\varepsilon_{y(2)}$ – in the second vertical wall with 2, 4 longitudinal reinforcement rods as well as average relative deformations $\varepsilon_{sz(1)}$ and $\varepsilon_{sz(2)}$ of the vertical rods of the clamps of the two walls, respectively.

Average relative deformations of longitudinal reinforcement in two vertical walls will be equal:

$$\varepsilon_{y(1)} = \frac{1}{2}\left(\frac{\sigma_{sy(1)}\psi_{sy(1)}}{E_S} + \frac{\sigma_{sy(3)}\psi_{sy(3)}}{E_S}\right);$$

$$\varepsilon_{y(2)} = \frac{1}{2}\left(\frac{\sigma_{sy(2)}\psi_{sy(2)}}{E_S} + \frac{\sigma_{sy(4)}\psi_{sy(4)}}{E_S}\right),$$

or, taking into account the values (29),

$$\varepsilon_{y(1)} = \frac{1}{2E_S}\left(\frac{\bar{N}_{sy(1)}\psi_{sy(1)}}{F_{S(1)}} + \frac{\bar{N}_{sy(3)}\psi_{sy(3)}}{F_{S(3)}}\right);$$

$$\varepsilon_{y(2)} = \frac{1}{2E_S}\left(\frac{\bar{N}_{sy(2)}\psi_{sy(2)}}{F_{S(2)}} + \frac{\bar{N}_{sy(4)}\psi_{sy(4)}}{F_{S(4)}}\right), \quad (44)$$

where the values of $\bar{N}_{sy(i)}$, $(i = 1,2,3,4)$ are determined by the dependencies (26) – (28).

The stresses in the vertical rods of the clamps are determined by the dependencies (9). Accordingly, the relative deformations will be:

$$\varepsilon_{sz(1)} = \frac{\sigma_{sz(1)}\psi_{sz(1)}}{E_S} = \frac{N_{yz(1)}\psi_{sz(1)}}{f_{sw}E_S\operatorname{tg}\infty_1};$$

$$\varepsilon_{sz(2)} = \frac{\sigma_{sz(2)}\psi_{sz(2)}}{E_S} = \frac{N_{yz(2)}\psi_{sz(2)}}{f_{sw}E_S\operatorname{tg}\infty_2}, \quad (45)$$

where the coefficients $\psi_{sz(1)}$ and $\psi_{sz(2)}$ are determined by dependence (31), where the index “y” is replaced by Z, the values $N_{yz(1)}$, $N_{yz(2)}$ are determined by the dependencies (5), (6).

By analogy with (37) – (41), the stresses $\sigma_{bt(1)}$ and $\sigma_{bt(2)}$ and the relative deformations $\varepsilon_{bt(1)}$ and $\varepsilon_{bt(2)}$ of concrete strips along the cracks in the vertical walls of the cross-sectional box of the element are determined.

$$\sigma_{bt(1)}=-2\tau_{yx}\sin\alpha_1\cos\alpha_1=-\frac{2N_{yx}\sin\alpha_1\cos\alpha_1}{2\alpha\beta_z};$$
$$\sigma_{bt(2)}=-2\tau_{yx}\sin\alpha_2\cos\alpha_2=-\frac{2N_{yx}\sin\alpha_2\cos\alpha_2}{2\alpha\beta_z};\tag{46}$$

$$\varepsilon_{bt(1)}=\frac{\sigma_{bt(1)}}{E_n\nu_{n(1)}}=-\frac{N_{yx}\sin\alpha_1\cos\alpha_1}{\alpha\beta_z E_n\nu_{n(1)}};$$
$$\varepsilon_{bt(2)}=\frac{\sigma_{bt(2)}}{E_n\nu_{n(2)}}=-\frac{N_{yx}\sin\alpha_2\cos\alpha_2}{\alpha\beta_z E_n\nu_{n(2)}},\tag{47}$$

where E_n is the modulus of deformation of concrete strips. determined from dependence (39), α and β_z are quantities similar to the quantities α, β_{xy}, f'_{sy} included in dependence (41), $\nu_{n(1)}$, $\nu_{n(2)}$ are coefficients that take into account the effect of plastic deformations of concrete strips on an increase in the total deformations $\varepsilon_{bt(1)}$ and $\varepsilon_{bt(2)}$.

By analogy with (43), the total shear angles in the first and second walls of the element will be equal:

$$\gamma_{yz(1)}=\varepsilon_{sz(1)}\mathrm{ctg}\alpha_1+\varepsilon_{y(1)}\mathrm{tg}\alpha_1+\frac{\varepsilon_{bt(1)}}{\sin\alpha_1\cos\alpha_1};$$
$$\gamma_{yz(2)}=\varepsilon_{sz(2)}\mathrm{ctg}\alpha_2+\varepsilon_{y(2)}\mathrm{tg}\alpha_2+\frac{\varepsilon_{bt(2)}}{\sin\alpha_2\cos\alpha_2},$$

or, taking into account (45), (47):

$$\gamma_{yz(1)}=\frac{N_{yz(1)}\psi_{sz(1)}}{f_{sw}E_S\mathrm{tg}\infty_1}\mathrm{ctg}\alpha_1+$$
$$+\frac{\mathrm{tg}\alpha_1}{2E_S}\left(\frac{\bar{N}_{sy(1)}\psi_{sy(1)}}{F_{S(1)}}+\frac{\bar{N}_{sy(3)}\psi_{sy(3)}}{F_{S(3)}}\right)+\frac{N_{yx}}{E_n\alpha\beta_z\nu_{n(1)}};$$
$$\gamma_{yz(2)}=\frac{N_{yz(2)}\psi_{sz(2)}}{f_{sw}E_S\mathrm{tg}\infty_2}\mathrm{ctg}\alpha_2+$$
$$+\frac{\mathrm{tg}\alpha_2}{2E_S}\left(\frac{\bar{N}_{sy(2)}\psi_{sy(2)}}{F_{S(2)}}+\frac{\bar{N}_{sy(4)}\psi_{sy(4)}}{F_{S(4)}}\right)+\frac{N_{yx}}{E_n\alpha\beta_z\nu_{n(2)}}.\tag{48}$$

The twisting angles, following [18], are determined through the values of the shear angles γ_{xy} and γ'_{xy} of the lower and upper surfaces according to (43) and $\gamma_{xz(1)}$, $\gamma_{xz(2)}$ of the first and second walls box-section of the element according to the constraints (48), after which

$$\varphi=\frac{b_1\left(\gamma_{xy}+\gamma'_{xy}\right)+h_1\left(\gamma_{xz(1)}+\gamma_{xz(2)}\right)}{2b_1h_1}.\tag{49}$$

The curvature of the element $\left(1/\rho_y\right)$ and relative deformations $\left(\varepsilon_{0y}\right)$ at the level of the y axis are determined from the dependencies

$$\frac{1}{\rho_y}=\frac{\varepsilon_{sy}-\varepsilon'_{sy}}{h_1};\qquad \varepsilon_{0y}=\frac{\varepsilon_{sy}+\varepsilon'_{sy}}{2}, \tag{50}$$

where ε_{sy}, ε'_{sy} are defined according to (33), (34).

Based on dependencies (3), (5), (6), (26) – (28), the twist angle, curvature and relative deformations at the levels of the y axis are expressed depending on M, T, N, Q.

3. Results and Discussion

The calculated dependences for determining the deformations and angles of rotation of the cross-sectional box of the element are constructed in such a way that the wall thickness of the section element is not limited and makes it possible to switch to a solid section. It should only be taken into account that in elements of a solid section, according to the data of experimental studies [20–21], after the formation of cracks, a part of the torque T_2 can be perceived by some solid core of the section that remains after cracking, and a part of the moment T_1 is perceived by the reinforcement in the section with a crack. In this case, for the application of the dependences obtained for the cross-sectional box when calculating the solid section in the formulas, the torque T is replaced by T_1. The values of the moments T_1, T_2 in relative values can be determined from the experimental “torque-angle of twisting” graphs [21]. As a first approximation, you can use the formula proposed in [18]:

$$T=T_1+T_2;\qquad T_1=T\left[1-0.3\left(\frac{T_{cr}}{T}\right)^4\right], \tag{51}$$

where T_{sr} is the torque at the moment of cracking, T is the current torque $\left(T>T\right)$.

In this case, the question of the expediency of taking into account the effect of the concrete core is determined by the ratio of the torque and bending moments, the presence and value of longitudinal forces in the section under consideration as shown by experimental studies. It is advisable to take this effect into account only in the presence of spiral cracks developing along the entire contour [21]. In the presence of concrete in the compressed zone without cracks, the effect of the concrete core can be neglected, assuming $T_2=0$.

4. Conclusions

1. The refined calculation model of the complex resistance of reinforced concrete structures of the cross-sectional box, experiencing the combined action of bending and torque moments, axial and transverse forces in the stage after the formation of spatial cracks, is proposed. This stage allows you to determine analytically the stresses in the concrete in the compressed zone, the height of the compressed concrete, the stresses in the clamps, the deformations in the compressed zone of concrete as well as in the longitudinal and transverse reinforcement rods, the curvature of the element and the angle of its twisting.
2. The given design dependencies take into account all the main external influences for a reinforced concrete rod element of the cross-sectional box: torsional (T) and bending (M) moments, transverse (Q) and axial (N) forces. In this case, the action of the torque and transverse force is reduced to the action of the flow of tangential forces along the rectangular contour of the section.
3. The developed model can be used in the design of a wide class of reinforced concrete structures of buildings and structures made of ordinary and high-strength concrete and fiber-reinforced concrete, experiencing complex stress state – torsion with bending and the action of axial forces.

References

1. Ali, A.H., Mohamed, H.M., Chalioris, C.E., Deifalla, A. Evaluating the shear design equations of FRP-reinforced concrete beams without shear reinforcement. Engineering Structures. 2021. 235. Article no. 112017. DOI: 10.1016/j.engstruct.2021.112017
2. Ban, H., Tan, E.L., Uy, B. Strength of multi-span composite beams subjected to combined flexure and torsion. Journal of Constructional Steel Research. 2015. 113. Pp. 1–12. DOI: 10.1016/j.jcsr.2015.05.023
3. Mostofinejad, D., Talaeitaba, S.B. Nonlinear Modeling of RC Beams Subjected to Torsion using the Smeared Crack Model. Procedia Engineering. 2011. 14. Pp. 1447–1454. DOI: 10.1016/J.PROENG.2011.07.182
4. Kalkan, I., Kartal, S. Torsional rigidities of reinforced concrete beams subjected to elastic lateral torsional buckling. International Journal of Civil and Environmental Engineering. 2017. 11(7). Pp. 969–972.
5. Arzamastsev, S.A., Rodevich, V.V. By the calculation of reinforced concrete elements under bend with torsion. Proceedings of higher educational institutions. Construction. 2015. 9. Pp. 99–109.
6. Gunasekaran, K., Ramasubramani, R., Annadurai, R., Prakash Chandar, S. Study on reinforced lightweight coconut shell concrete beam behavior under torsion. Materials and Design. 2014. 57. Pp. 374–382. DOI: 10.1016/j.matdes.2013.12.058
7. Rahal, K.N. A unified approach to shear and torsion in reinforced concrete. Structural Engineering and Mechanics. 2021. 77(5). Pp. 691–703. DOI: 10.12989/sem.2021.77.5.691
8. Bernardo, L.F.A., Andrade, J.M.A. A unified softened truss model for RC and PC beams under torsion. Journal of Building Engineering. 2020. 32. Article no. 101467. DOI: 10.1016/j.jobe.2020.101467
9. Bernardo, L.F.A., Andrade, J.M.A., Nunes, N.C.G. Generalized softened variable angle truss-model for reinforced concrete beams under torsion. Materials and Structures. 2015. 48(7). Pp. 2169–2193. DOI: 10.1617/s11527-014-0301-z
10. Jafari, F., Akbari, J. Reliability-based design of reinforced concrete beams for simultaneous bending, shear, and torsion loadings. Frattura ed Integrita Strutturale. 2020. 14(51). Pp. 136–150. DOI: 10.3221/IGF-ESIS.51.11
11. Rahal, K. Combined Torsion and Bending in Reinforced and Prestressed Concrete beams Using Simplified Method for Combined Stress-Resultants. ACI Structural Journal. 2007. 104(4). Pp. 402–411.
12. Thomas, A., Hameed, A.S. An Experimental Study on Combined Flexural and Torsional Behaviour of RC Beams. International Research Journal of Engineering and Technology. 2017. 4(5). Pp. 1367–1370. DOI: 10.13140/RG.2.2.19425.51045
13. Behera, G.C., Rao, T.D.G., Rao, C.B.K. Torsional behaviour of reinforced concrete beams with ferrocement U-jacketing – Experimental study. Case Studies in Construction Materials. 2016. 4. Pp. 15–31. DOI: 10.1016/j.cscm.2015.10.003
14. Ajeel, A.E. Torsion plus bending and shear on reinforced concrete beams. Journal of Engineering and Sustainable Development. 2016. 20(4). Pp. 277–878.
15. Al-Bayati, G., Kalfat, R., Al-Mahaidi, R., Hashemi, J. Experimental study on crack propagation of CFRP-strengthened RC beams subjected to torsion. Australian Journal of Structural Engineering. 2018. 19(4). Pp. 279–297. DOI: 10.1080/13287982.2018.1523293
16. Jariwala, V.H., Patel, P.V., Purohit, S.P. Strengthening of RC beams subjected to combined torsion and bending with GFRP composites. Procedia Engineering. 2013. 51. Pp. 282–289. DOI: 10.1016/j.proeng.2013.01.038
17. Lee, J.H., Park, Y.M., Jung, C.Y. et al. Experimental and Measurement Methods for the Small-Scale Model Testing of Lateral and Torsional Stability. International Journal of Concrete Structures and Materials. 2017. 11. Pp. 377–389. DOI: 10.1007/s40069-017-0198-3
18. Karpenko, N.I., Kolchunov, Vl.I., Travush, V.I. Calculation model of a complex stress reinforced concrete element of a boxed section during torsion with bending. Russian journal of building construction and architecture. 2021. 3(51). Pp. 7–26. DOI: 10.36622/VSTU.2021.51.3.001
19. Kolchunov, V.I., Dem'yanov, A.I. The modeling method of discrete cracks in reinforced concrete under the torsion with bending. Magazine of Civil Engineering. 2018. 81(5). Pp. 160–173. DOI: 10.18720/MCE.81.16
20. Demyanov, A.I. Crack formation in high-strength reinforced concrete structures at complex resistance – torsion with bending. Building and Reconstruction. 2019. 5. Pp. 3–10. DOI: 10.33979/2073-7416-2019-85-5-3-10
21. Travush, V.I., Karpenko, N.I., Kolchunov, V.I., et al. Main results of experimental studies of reinforced concrete structures of high-strength concrete B100 round and circular cross sections in torsion with bending. Structural Mechanics of Engineering Constructions and Buildings. 2019. 15(1). Pp. 51–61. DOI: 10.22363/1815-5235-2019-15-1-51-61
22. Kumar, C.A., Mohan, M., Rajesh, D.V.S.P., Kulkarni, P. Behavior of fibre reinforced concrete beam in combined bending and torsion. International Journal of Research in Engineering and Technology. 2015. 4. Pp. 450–455.
23. Jog, C.S., Imrankhan, S.M. A finite element method for the Saint-Venant torsion and bending problems for prismatic beams. Computers & Structures. 2014. 135. Pp. 62–72. DOI: 10.1016/j.compstruc.2014.01.010
24. Nguyen, T.A., Nguyen, Q.H., Somja, H. Nonlinear analysis of RC members subjected to combined bending–shear–torsion stresses: a numerical multi-fiber displacement-based finite element model with warping. Acta Mechanica. 2021. 232(3). Pp. 2635–2658. DOI: 10.1007/s00707-021-02966-x
25. Nguyen, T.A., Nguyen, Q.H., Somja, H. An enhanced finite element model for reinforced concrete members under torsion with consistent material parameters. Finite Elements in Analysis and Design. 2019. 167. Article no. 103323. DOI: 10.1016/j.finel.2019.103323
26. Bulkin, S.A. Torsion with bending of rectangular steel fiber reinforced concrete beam. Building and Reconstruction. 2021. 2. Pp. 3–13.
27. Karpenko, N.I., Kolchunov, Vl.I., Kolchunov, V.I., Travush, V.I., Dem'yanov, A.I. Deformation of reinforced concrete structures during bending with torsion. Stroitel'nye Materialy (Construction Materials Russia). 2021. 6. Pp. 47–56. DOI: 10.31659/0585-430X-2021-792-6-48-56

Information about the authors:

***Nickolay Karpenko**, Doctor of Technical Sciences*
E-mail: niisf_lab9@mail.ru

***Sergey Karpenko**, Doctor of Technical Sciences*
E-mail: niisf@niisf.ru

***Vladimir Kolchunov**, Doctor of Technical Sciences*
ORCID: https://orcid.org/0000-0001-5075-1134
E-mail: vlik52@mail.ru

***Vitaly Kolchunov**, Doctor of Technical Sciences*
E-mail: asiorel@mail.ru

Received: 02.10.2021. Approved after reviewing: 09.07.2024. Accepted: 09.07.2024.